Deterministic escape dynamics of two-dimensional coupled nonlinear oscillator chains

S. Fugmann,[1] D. Hennig,[1] L. Schimansky-Geier,[1] and P. Hänggi[2]
[1]*Institut für Physik, Humboldt-Universität Berlin, Newtonstrasse 15, 12489 Berlin, Germany*
[2]*Institut für Physik, Universität Augsburg, Universitätsstrasse 1, 86135 Augsburg, Germany*
(Received 14 December 2007; revised manuscript received 7 March 2008; published 26 June 2008)

We consider the deterministic escape dynamics of a chain of coupled oscillators under microcanonical conditions from a metastable state over a cubic potential barrier. The underlying dynamics is conservative and noise free. We introduce a two-dimensional chain model and assume that neighboring units are coupled by Morse springs. It is found that, starting from a homogeneous lattice state, due to the nonlinearity of the external potential the system self-promotes an instability of its initial preparation and initiates complex lattice dynamics leading to the formation of localized large amplitude breathers, evolving in the direction of barrier crossing, accompanied by global oscillations of the chain transverse to the barrier. A few chain units accumulate locally sufficient energy to cross the barrier. Eventually the metastable state is left and either these particles dissociate or pull the remaining chain over the barrier. We show this escape for both linear rodlike and coil-like configurations of the chain in two dimensions.

DOI: 10.1103/PhysRevE.77.061135 PACS number(s): 05.40.−a, 05.45.−a, 63.20.Pw, 63.20.Ry

I. INTRODUCTION

The problem of escape from metastable states is omnipresent in diverse scientific areas ranging from chemical kinetics [1], diffusion in solids [2], nucleation [3] to electrical transport [4], to name only a few. Theoretical models describing escape in theses systems widely exploit that the barrier crossing can be well described by the Brownian motion of a reaction coordinate in a potential well, as proposed by Kramers in the 1940s [5,6]. There it is implied that the system is in contact with an external heat bath serving as a permanent source of energy, causing dissipation and local energy fluctuations which successfully enable the escapes. These models with thermally activated barrier crossings were and are consecutively in the focus of numerous important studies [7–9]. Many generalizations of Kramers escape theory in overdamped and underdamped versions have been widely exploited [7]. Starting from one-dimensional models the theory of thermally activated escape has been generalized to systems with many degrees of freedom; the first works date back to the late 1960s [9], for evolutionary processes [10], and particularly as well in the biophysical context such as the transport of long and flexible polymers across membranes and DNA electrophoresis [11–16].

Less intensely the noise-free microcanonical situation has been studied, where the system cannot feed on an external energy source but rather a fixed amount of energy must suffice to perform a barrier crossing. Such deterministic process of a one-dimensional coupled oscillator chain has been presented as a robust—and purely self-organized—barrier crossing mechanism [17,18]. The absolutely necessary ingredients in the physics of these deterministic escapes are nonlinear potentials wherein the chain moves and the discreteness of the chain units. Both avert the chain to relax to states with equipartition of energy among its constituents. In contrast they allow for localization of a sufficient amount of energy on a few oscillators forming a critical state. Gathering overcritical energy these few units pull the whole chain across the barrier [17,18]. Possibly, they dissociate from the chain carrying their energy away.

Thus, providing only a small amount of energy initially homogeneously to the system, discreteness and nonlinearity conspire into producing strongly localized lattice states, enabling the system to pass critical equilibrium configurations, so-called transition states [19]. These intrinsic localized modes, also referred to as discrete breather*s*, have become more and more of interest in a variety of physical systems in recent years [20–29].

As an extension to the one-dimensional chain system [17,18] we introduce a two-dimensional chain model with pairwise nonlinear Morse interaction and study the influence of the additional degree of freedom on the self-organized escape process. In contrast to the previous study taking into account solely motion in the transition direction, this time motion is also allowed transverse to the barrier along the well of the external potential. In consequence, in addition to the formation of localized large amplitude breathers, with amplitudes evolving in transition direction, global oscillations of the chain transverse to the barrier are observed. Eventually a few chain links accumulate locally sufficient energy to cross the barrier. This mechanism is shown to take place for both linear rodlike and for coil-like configurations of the chain in two dimensions (2D).

In the following section we show details of this deterministic escape. We introduce the two-dimensional coupled oscillator chain model and discuss in Sec. III the modulational instability being responsible for localization of energy in the chain. In Sec. IV we pay special interest to the formation of acoustic modes transverse to the direction of barrier crossing and their influence on the escape process is studied. Related to the latter we present in Sec. V the critical chain configurations referred to as the transition states. We proceed in Sec. VI by examining the parameter dependence of the escape statistics of the oscillator chain. To conclude we summarize our results.

II. TWO-DIMENSIONAL COUPLED OSCILLATOR CHAIN MODEL

Our study treats a spring mass chain model. The chain consists of N oscillators—also referred to as units—which

are pairwise connected through nonlinear springs. The motion of these units takes place in the x-y plane. We denote by q_{xn} the displacement of the nth oscillator in the x direction also referred to as the transition coordinate while in the transverse y-direction displacements from the rest position are denoted by q_{yn}. The local on-site potential U reads as

$$U(q_{xn},q_{yn}) = \frac{m\omega_0^2}{2}q_{xn}^2 - \frac{a}{3}q_{xn}^3, \tag{1}$$

with $n=1,\ldots,N$. It obeys a cubic nonlinearity in one space direction and is flat in the transverse one, hence the potential landscape has the shape of an eaves gutter, shown in Figs. 1 and 2. The potential possesses a metastable equilibrium at $q_x^{\min}=0$, corresponding to the rest energy $E_{\min}=0$ and the maximum is located at $q_x^{\max}=m\omega_0^2/a$ with energy $E_{\max} \equiv \Delta E=m^3\omega_0^6/(6a^2)$. Thus, in order for units to escape from the potential well of depth ΔE over the energy barrier and subsequently into the range $q_x > q_x^{\max}$ a sufficient amount of energy must be supplied.

We assume a nonlinear interaction potential of Morse type between adjacent entities of the chain

$$U_M(r_{n+1,n}) = D_0(1-e^{-d(r_{n+1,n}-l)})^2, \tag{2}$$

with depth D_0, range parameter d, l the equilibrium distance of the oscillators (also referred to as bond length), and $r_{n+1,n}$ the Euclidean distance of two neighboring oscillators,

$$r_{n+1,n} = \sqrt{(q_{xn+1}-q_{xn})^2 + (q_{yn+1}-q_{yn})^2}, \tag{3}$$

with $n=1,\ldots,N-1$.

The Hamiltonian of the two-dimensional chain model reads as

$$H = \sum_{n=1}^{N}\left(\frac{p_{xn}^2}{2m} + \frac{p_{yn}^2}{2m} + U(q_{xn},q_{yn})\right) + \sum_{n=1}^{N-1} U_M(r_{n+1,n}). \tag{4}$$

From that Hamiltonian we derive the Hamilton equations $\dot{q}_{xn}=\partial H/\partial p_{xn}$ and $\dot{p}_{xn}=-\partial H/\partial q_{xn}$ for the canonically conjugated variables in the x direction and accordingly in the y direction. By rescaling space $\tilde{q}=dq$, conjugated momentum $\tilde{p}=dp/(m\omega_0)$ and time $\tilde{t}=\omega_0 t$, furthermore introducing $\tilde{a}=a/(dm\omega_0^2)$ and $\kappa=2D_0d^2/(m\omega_0^2)$ and neglecting in the following the tilde in our notation we pass to dimensionless variables.

a is called the anharmonicity parameter determining the ratio of nonlinear and linear force terms associated with the local on-site potential. The now dimensionless energy is $\tilde{E}=d^2/(m\omega_0^2)E$. The value of the barrier energy is thus

$$\Delta E = \frac{1}{6a^2}. \tag{5}$$

For further investigations we introduce the important intrinsic length scale

$$s = q_x^{\max} - q_x^{\min} = \frac{1}{a}. \tag{6}$$

The dynamics of the chain will be crucially affected by the ratio l/s, i.e., the ratio of the bond length and the intrinsic length scale s of the system. Small ratios cause coil-like chain configurations, while rodlike states appear for ratios of the order of one or above. Note that in the limit of vanishing a the barrier disappears and the intrinsic length scale diverges.

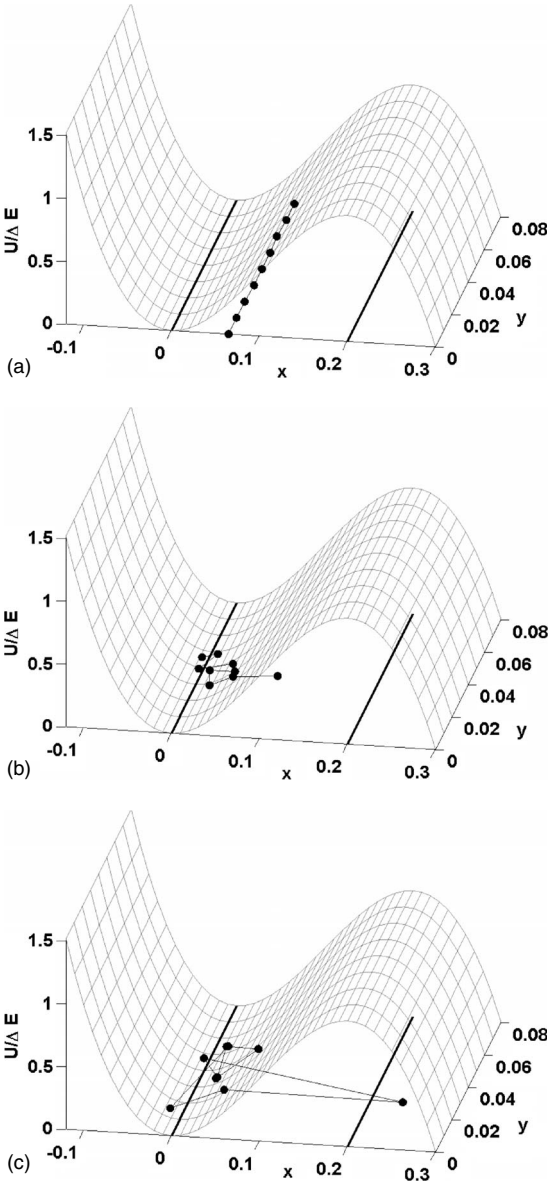

FIG. 1. Coil-like structures, $l/s<1$. Snap shots of the dynamics illustrating the formation of localized structures with a subsequent barrier crossing event in the limit of weak coupling and short bond length, for one realization of initial conditions. The initial conditions are $q_{x0}=0.065$ and $\Delta q_x=0.001$, yielding $E_0/\Delta E=0.248$. The remaining parameter values are $a=5$, $\kappa=0.15$, $l/s=0.05$, and $N=9$. (a) Snap shot taken at time $t=0$, initially virtually flat state. (b) Snap shot taken at time $t=210$, the chain has coiled and a localized state in the x direction has formed. (c) Snap shot taken at time $t=655$, one unit has overcome the barrier level. Subsequently this unit escapes while the remaining oscillators stay captured inside the potential well (not shown here). The solid lines in the x-y plane designate the position of the potential's minimum and maximum.

The equations of motion derived from the Hamiltonian (4) read as

$$\ddot{q}_{xn} = -q_{xn} + a\, q_{xn}^2 - \kappa(1 - e^{-(r_{n+1,n}-l)})e^{-(r_{n+1,n}-l)}\frac{q_{xn} - q_{xn+1}}{r_{n+1,n}}$$

$$- \kappa(1 - e^{-(r_{n,n-1}-l)})e^{-(r_{n,n-1}-l)}\frac{q_{xn} - q_{xn-1}}{r_{n,n-1}}, \quad (7)$$

$$\ddot{q}_{yn} = -\kappa(1 - e^{-(r_{n+1,n}-l)})e^{-(r_{n+1,n}-l)}\frac{q_{yn} - q_{yn+1}}{r_{n+1,n}}$$

$$- \kappa(1 - e^{-(r_{n,n-1}-l)})e^{-(r_{n,n-1}-l)}\frac{q_{yn} - q_{yn-1}}{r_{n,n-1}}, \quad (8)$$

for $n=2,\ldots,N-1$. We impose open boundary conditions. Hence for $n=1$ ($n=N$) the coupling force to the left-hand (right-hand) neighbor vanishes. For our studies we fix the parameter value of the local on-site potential by setting $a=5$.

Focusing our interest on a flat initial state as sketched in the panel (a) of Figs. 1 and 2, small perturbations on the corresponding plane elongation with amplitude q_{x0} are included taking random initial amplitudes which are uniformly distributed in an interval $|q_{xn}(0)-q_{x0}| \leq \Delta q_x$.

The mean values of q_{x0} are taken in such a way that the average excitation energy of a single oscillator, E_0, is small compared to the depth, ΔE, of the potential well. Due to the choice of sufficiently small displacements Δq_x the initial lattice state, $q_{xn}(0)=q_{x0}+\Delta q_{xn}$, is close to an almost homogeneous state and yet sufficiently disturbed that there result small but nonvanishing initial interaction terms. Thus an energy exchange between the coupled units is entailed. The initial momenta $\{p_{xn}(0)\}=0$ are set zero. The initial amplitudes in the transverse direction are $q_{yn}(0)=nl$ and the momenta $\{p_{yn}(0)\}=0$ are zero, implying the conservation of the center of mass in the y direction.

If in the beginning the energy is virtually equally shared among all units in the chain, expressed by a homogeneous elongation of the whole chain in the transition direction as shown in the panel (a) of Figs. 1 and 2, the escape scenario is the following: After a certain time has evolved, the uniform state is disturbed and energy gets localized [panel (b) in Figs. 1 and 2, each showing a snap shot of a typical amplitude dynamics for two different parameter sets, for details see the captions]. Eventually at least one unit possesses enough energy to overcome the barrier [panel (c) in Figs. 1 and 2]. Whether a cascade of barrier crossings is initiated depends on the bond length as well as on the value of the coupling strength. In the limit of $l/s \to 0$—that means small bonds compared to the width of the local potential—and a weak coupling (corresponding to the snap shots presented in Fig. 1) the chain tends to fragment. Whereas for longer bonds $l/s > 1$ and a stronger coupling (see Fig. 2, notice the change of the y scale compared to the previous figure), the unit that has overcome the barrier, pulls its neighbors over the latter. Consequently, concerted escape of the entire chain from the potential valley becomes possible.

The amplitudes of escaped units are kept fixed after passing a threshold far behind the barrier, which we chose as $q_x^{\text{thresh}} = 100 q_x^{\max}$.

Numerical schemes. We have numerically integrated the set of Eqs. (7) and (8) with an explicit fourth-order symplectic integrator scheme [30]. The accuracy of the calculation was checked by continuously monitoring numerically the conservation of the total energy with a precision of at least $|[E(t)-E(0)]/E(0)| = 10^{-9}$. We tested also alternative numeri-

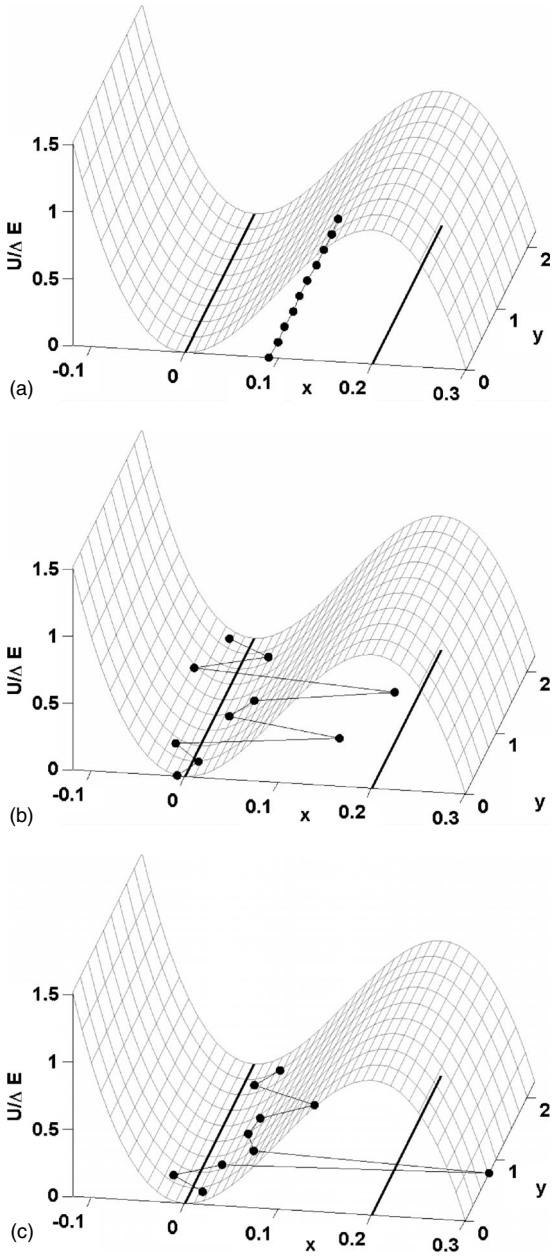

FIG. 2. Rod-like structures, $l/s > 1$. Snap shots of the dynamics illustrating the formation of localized structures with a subsequent barrier crossing event, for one realization of initial conditions. The initial conditions are $q_{x0}=0.09$ and $\Delta q_x = 0.001$, yielding $E_0/\Delta E = 0.425$. The remaining parameter values are $a=5$, $\kappa=0.9$, $l/s = 1.25$, and $N=10$. (a) Snap shot taken at time $t=0$, initially virtually flat state. (b) Snap shot taken at time $t=235$, a short wavelength amplitude pattern (π mode) in the x direction has appeared. (c) Snap shot taken at time $t=245$, one unit has overcome the barrier level. Subsequently the whole chain escapes (not shown here). The solid lines in the x-y plane designate the position of the potential's minimum and maximum.

cal integration schemes, such as an explicit Runge-Kutta scheme of fourth order and an implicit Runge-Kutta scheme. In all cases we found identical results. More precisely, starting with the same initial conditions (and always imposing the same boundary conditions) and using the above-mentioned integration schemes, for all of these numerical schemes we reproduced over a time interval of 10^6 time units identical results for the trajectories.

Moreover, we confirmed that our numerical results are insensitive to the step size of the employed integrator. We emphasize that even in cases when the amplitudes of some of the oscillators grow significantly (i.e., the formation of large amplitude breathers) the numerical accuracy was assured by monitoring the conservation of energy. Because the explicit symplectic integration scheme yields results identical to those obtained with a numerically stable implicit integrator we conclude that our results are numerically stable.

In addition the preservation of the total momentum along the transverse direction, where the system is translation invariant, is also guaranteed. The following sections deal with the main stages of the coupled dynamics culminating in the self-organized deterministic escape process.

III. MODULATIONAL INSTABILITY

It is well know that the formation of localized excitations in nonlinear systems can be caused by modulational instability [27–29,31,32]. This mechanism initiates an instability of a plane wave when small perturbations of nonvanishing wave numbers are imposed.

We underline that we focus our interest on a virtually flat initial state. Then, the growth rate of perturbations with wave number $K \in [-\pi, \pi]$ in the limit of large bond length $l \gtrsim O(s)$, $l \gg \Delta q_x$, is given by

$$\Gamma \simeq \sqrt{\kappa \frac{(\Delta q_x)^2}{l^2} \frac{10a^2 q_{x0}^2}{3} \sin^2\left(\frac{K}{2}\right)} + O(\tilde{\kappa}). \tag{9}$$

A derivation of Eq. (9) is presented in the Appendix.

In the weakly nonlinear regime—i.e., $E_0 \simeq q_{x0}^2/2$—we can rewrite Eq. (9) in a more convenient form involving the ratio of the average excitation energy and the barrier height

$$\Gamma \simeq \sqrt{\kappa \frac{(\Delta q_x)^2}{l^2} \frac{10E_0}{9\Delta E} \sin^2\left(\frac{K}{2}\right)}. \tag{10}$$

According to this equation all perturbing modes taken from the first Brillouin zone are unstable. The maximum growth rate is found at $|K_{\max}| = \pi$. Indeed the structures presented in the panel (b) of Fig. 2 and in the panel (b) of Fig. 3 have this characteristic, that is there arises an array consisting of numerous breathers. Moreover, from Eq. (9) we can infer that the growth rate of small amplitude perturbations shrinks with enlarging bond length l. That means it takes longer times for the creation of localized structures. The other way around, the rate grows with increasing amplitude of the initial elongation. We note that such short wavelength localized structures experience no modification when the number of chain units, N, is varied.

With concern to the limit of short bond lengths $l \to 0$, where (9) does not apply, we observe the formation of a long wavelength ($|K_{\max}| < \pi$) localized structure similar to the one that has been observed in [17,18]. Provided that the size of the chain is large compared to the wavelength of the localized structures, i.e., $N > 2\pi/K_{\max}$, these structures—and in particular their wavelength—are not affected when changing the number of chain units N. The formation of an array of localized solutions (large-amplitude breathers) in the x direction is illustrated in the panel (a) of Fig. 3. We remark that an increase of the coupling strength enlarges the typical wavelength of the structure [18].

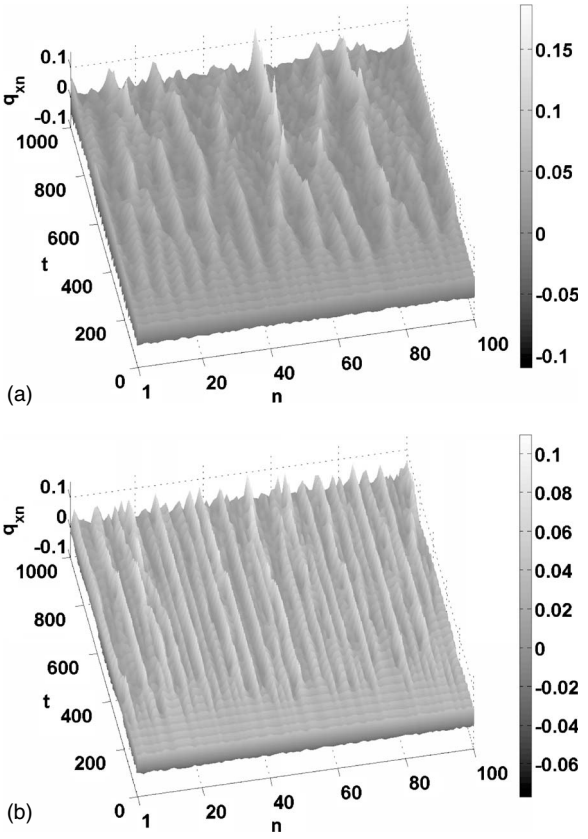

FIG. 3. Formation of localized structures. Depicted are the spatiotemporal evolutions of the amplitudes $\{q_{xn}\}$ for each one realization of initial conditions. (a) $l/s < 1$, formation of an array of localized solutions (large-amplitude breathers). The initial conditions are $q_{x0}=0.04$ and $\Delta q_x=0.001$, yielding $E_0/\Delta E=0.104$. The remaining parameter values are $a=5$, $\kappa=0.15$, $l/s=0.05$, and $N=100$. (b) $l/s > 1$, formation of an array consisting of numerous breathers. The initial conditions are $q_{x0}=-0.05$ and $\Delta q_x=0.001$, yielding $E_0/\Delta E=0.219$. The remaining parameter values are $a=5$, $\kappa=0.5$, $l/s=2.0$, and $N=100$.

Note, that, despite the presence of a nonlinear intersite interaction, the situation must be distinguished from the well-known Fermi-Past-Ulam model [33]. In our model the instability of the initial lattice state is solely governed by the nonlinearity of the on-site potential.

IV. ENERGY REDISTRIBUTION PROCESS

The process of modulational instability governs the dynamics of the system at an early instant of time. Later on, the

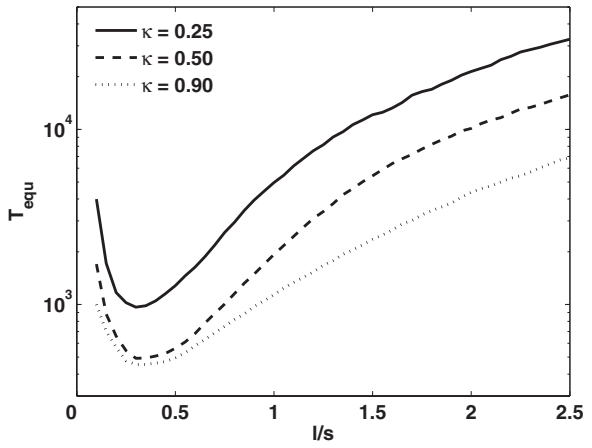

FIG. 4. Mean time T_{equ} in which an equipartition of energy is reached as a function of the bond length l. Values of the coupling strength as depicted in the legend. The initial conditions are $q_{x0}=-0.04$ and $\Delta q_x=0.001$, yielding $E_0/\Delta E=0.136$. The remaining parameter values are $a=5$ and $N=100$.

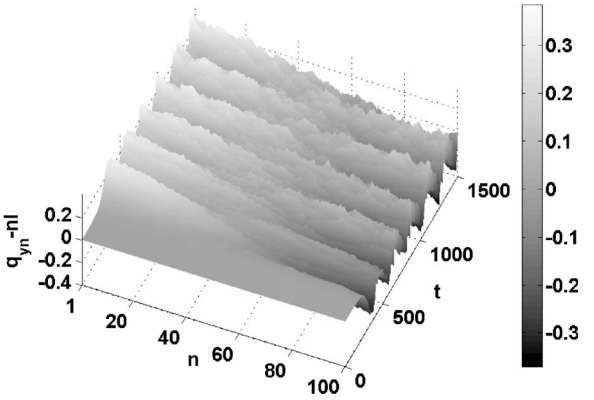

FIG. 5. Global oscillations in the y direction. Shown is the spatiotemporal evolution of the amplitudes $\{q_{yn}\}$ for one realization of initial conditions. The amplitude values are shifted with respect to their initial values nl. The initial conditions are $q_{x0}=-0.05$ and $\Delta q_x=0.001$, yielding $E_0/\Delta E=0.219$. The remaining parameter values are $a=5$, $\kappa=0.9$, $l/s=1.25$, and $N=100$.

influence of the—compared to a purely one-dimensional oscillator model—second, transverse, degree of freedom is expected to crucially affect the dynamical processes of the coupled oscillator chain.

Interestingly, we observe that in the cases of very short bond lengths $l/s \ll 1$ and bond lengths fulfilling $l/s > 1$ the structure, which is formed by modulational instability, persists for very long times, whereas it disappears rather fast for bond length values in between.

Such decrease of the amplitudes of the localized structures in the x direction comes along with the excitation of motions in the transverse degree of freedom. As one measure for the energy content in the x and the y direction the respective kinetic energy can be taken. Initially the mean of the kinetic energy of the x motion is $E^x_{\mathrm{kin}}=0.5E_{\mathrm{total}}$, whereas $E^y_{\mathrm{kin}}=0$. Induced by the breather formation in the x direction an enhanced interaction of neighboring oscillators is caused and since the interaction force couples the motion in the x and in the y motion an energy transfer is initiated.

We assume that the system has reached a state of equipartition if $E_{\mathrm{kin}}=0.25E_{\mathrm{total}}$ in both the x and the y direction, respectively. In Fig. 4 we depict the mean times of attainment of the equipartitioned state as a function of the bond length for different values of the coupling strength. Averages are performed over 200 realizations of random initial conditions. Apparently this time shrinks with increasing coupling strength. We underline, that the energy transfer described above is a purely nonlinear effect. We never observed a complete back transfer of energy from the y to the x motion. In contrast, in [34] resonant regimes of periodic energy transfer in a two-dimensional one-particle system are reported. It is still an open question, why there exist no such resonant regions in the extended two-dimensional chain model.

For one realization of initial conditions the spatiotemporal evolution of the amplitudes $\{q_{yn}(t)\}$ is shown in Fig. 5. The parameter values are taken as $l/s=1.25$ and $\kappa=0.9$. The average excitation energy of a single unit is $E_0=0.219\Delta E$. We observe a breathinglike behavior, the chain contracts and relaxes along its axis periodically in time. (This behavior of global oscillations of the chain as a whole along the transverse direction should not be confused with the large-amplitude breathers evolving in the transition coordinate direction involving fairly strong energy localization at certain sites.) For the chosen set of parameters we obtain a period of about $T=216$. We find that the frequency of the global oscillation increases with growing coupling strength according to $\nu \propto \sqrt{\kappa}$. Furthermore, we find that the stronger the coupling strength the faster the higher-energy modes are excited and thus—in good agreement with the results obtained above—the relaxation process is accelerated.

V. TRANSITION STATES

Whether an oscillator involved in a large amplitude breather state is able to escape from the region of bounded motion inside the potential well or is held back depends on the corresponding amplitude pattern as well as on the coupling strength κ. The associated critical chain configuration—called the transition state—is determined by $\{\dot{q}_{xn}\}=\{\dot{q}_{yn}\}=0$ and $\{\dot{p}_{xn}\}=\{\dot{p}_{yn}\}=0$. Hence we look for an appropriate solution of the corresponding stationary system which represents a force-free configuration yielding a first-order saddle point in configuration space.

In order to calculate the transition state we apply a multidimensional root finding algorithm using the Newton-Raphson method. For an identified transition state we compute the eigenvalues of the corresponding Jacobian assuring that we indeed found a first-order saddle point on the energy surface.

In the following we consider two scenarios: The peak of the localized amplitude profile of the critical configuration is situated either at one free end of the chain (referred to as boundary critical localized mode—BCLM), or somewhere in between the free ends (referred to as CLM).

We first discuss the stationary solutions obtained for the CLMs. Figure 6 shows the amplitude profiles for two differ-

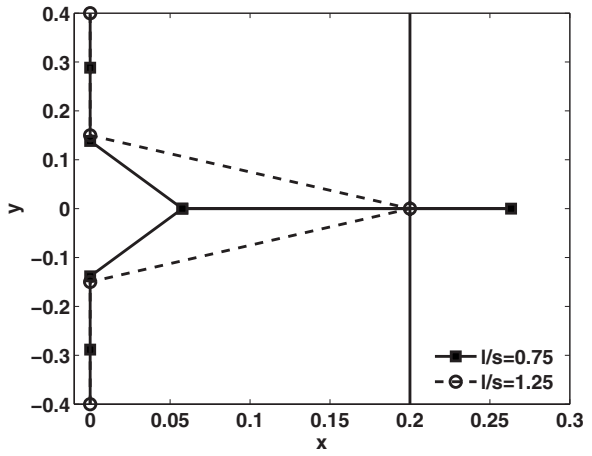

FIG. 6. Amplitude profiles of the CLM, centered at $y=0$ for two different bond lengths: $l/s=0.75$ (solid line with square symbols) and $l/s=1.25$ (dashed line with circles). For better illustration we depict only a segment of the chain, containing 5–7 units. The parameter values are $a=5$, $N=100$, and $\kappa=0.8$. The alignment of the units along the potential minimum situated at $q_x^{\min}=0$ is completely arbitrary, as long as next neighbors keep their equilibrium distance l. In particular, completely coiled configurations can be critical transition states.

ent values of l and a fixed coupling strength $\kappa=0.8$. We must distinguish two situations: First, $l<s$, represented by the critical profile with solid lines in Fig. 6. This profile resembles a thin needle with the central unit situated beyond the barrier. Here we must remark, that in general, the smaller the bond length l the larger is the extension of the critical localized mode along the x direction and the more oscillators are elongated from the potential's minimum. In contrast, for $l>s$, the central oscillator is always situated at the barrier, while its neighbors are arranged in such a way that there remains no stress arising from the bonds. We underline that the ends of the chain are free and there act thus no restoring forces. Hence, in order to reduce the stress arising from the elongation of the central oscillator over the barrier, its neighbors can be replaced force free along the y axis. Furthermore, due to the strong degree of localization the obtained structures remain the same when increasing the number of oscillators in the chain. We remark that the alignment of the units along the potential minimum situated at $q_x^{\min}=0$ is completely arbitrary, as long as next neighbors keep their equilibrium distance l. In particular, completely coiled configurations can be critical transition states, too.

For the BCLMs, the qualitative dependencies on the system's parameters κ and l remain—compared to the situation when the critical peak is formed between the ends—the same. But—since the oscillator beyond the barrier is now connected to only one neighbor inside the potential well and thus the acting back-pulling forces are smaller—the force-free critical state is less elongated.

For a critical chain configuration $\{\hat{q}_c\}$ the activation energy is determined by the following functional:

$$E_{\mathrm{act}}=\sum_{n=1}^{N}U(\hat{q}_{xn},\hat{q}_{yn})+\sum_{n=1}^{N-1}U_M(\hat{r}_{n+1,n}). \tag{11}$$

Concerning the dependence of the activation energy on the bond length, we observe a decay of E_{act} with enlarging bond length. In the limit $l\to s$ its value approaches $E_{\mathrm{act}}/\Delta E=1$. We remark that in the case of $l\geq s$ we always find a critical stationary solution with activation energy $E_{\mathrm{act}}=\Delta E$.

Provided that $l<s$, the activation energy E_{act} grows with an increasing value of the coupling strength. The growth is the stronger the smaller is l.

In the case of boundary critical localized modes the activation energies are remarkably lower compared to transition states with a peak somewhere in between the loose ends. A detailed analysis of the energetic contributions to the activation energy reveals that the major part of E_{act} is stored as deformation energy of the springs. Since a BCLM contains fewer stretched springs, the value of activation energy is lower.

We conclude that the process of barrier crossing of the chain is not only influenced by the amount of energy provided to the system. It also depends on the ratio of different length scales, since the geometry plays a crucial role for motions in a two-dimensional potential landscape. Thus, the rate of escape will be crucially affected by the choice of parameters.

VI. INFLUENCE OF THE PARAMETERS ON THE ESCAPE STATISTICS

In order to locate a parameter region where escape happens as fast as possible we study the escape statistics as a function of the coupling strength κ and the bond length l. We define the escape time of a chain as the moment at which the last escaped unit (the escape time of a single unit is denoted by t_{esc}) passes through the value $q_x^{\mathrm{thresh}}=100q_x^{\max}$ beyond the barrier. Performing averages of the escape time of a chain over hundreds of realizations of random initial conditions we compute the mean escape time T_{esc}. We fix the number of units to $N=100$.

In the following we focus our interest on parameter regions yielding an escape of the entire chain.

In order to illustrate the escape process, we depict in Fig. 7 the escape times t_{esc} versus the position of the escaping unit when the corresponding unit passes q_x^{thresh}. First, one unit moves directly beyond the barrier (since the underlying dynamics is irregular for different realizations of initial conditions the incident escape can happen at an arbitrary location in the chain) and in consequence adjacent units are subjected to pulling forces and a cascade of escapes is initiated in a relatively short time interval.

A. Coupling strength influence on the escape process

Our simulation time was set to $t_{\mathrm{sim}}=10^4$, corresponding to more than 1500 of linear ground-state oscillations. We calculate the fraction of positive escape events of the entire chain in relation to the number of simulations (200 realizations of initial conditions). Since not all simulations lead to

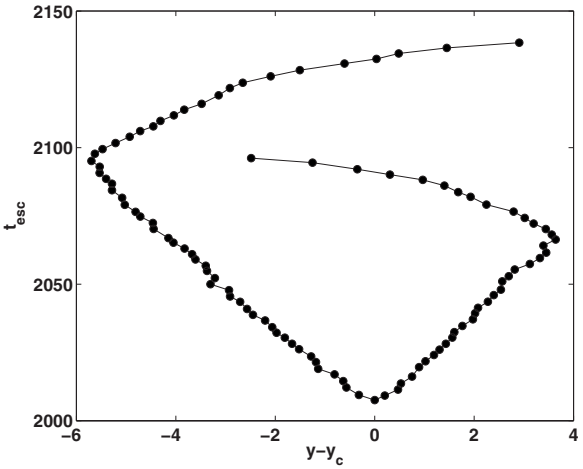

FIG. 7. Illustration of the escape process for one realization of initial conditions. The individual escape times t_{esc} versus the y position when the corresponding unit passes the threshold value q_x^{thresh} far behind the barrier. The position of the unit which overcomes the barrier first is denoted by y_c, all other positions are shifted by this value. The initial conditions are $q_{x0}=-0.05$ and $\Delta q_x=0.001$, yielding $E_0/\Delta E=0.219$. The parameter values are $a=5$, $\kappa=0.9$, $l/s=1.25$, and $N=100$.

positive escape events during t_{sim} the calculation of a mean escape time alone is not suitable.

In Fig. 8 we present the fraction of successful exits of the entire chain for two different bond lengths as a function of the coupling strength κ. The values of the bond lengths are chosen in such way that one is smaller and one is larger than s. For $\kappa=0.45$ we observe the first rare events of escape of the complete oscillator chain. The fraction of successful escape events of the entire chain further increases with enhanced coupling strength.

Whereas for the larger bond length at $\kappa=0.75$ the curve saturates to 1—i.e., all initial preparations lead to an escape of the whole chain—the curve for the smaller bond length

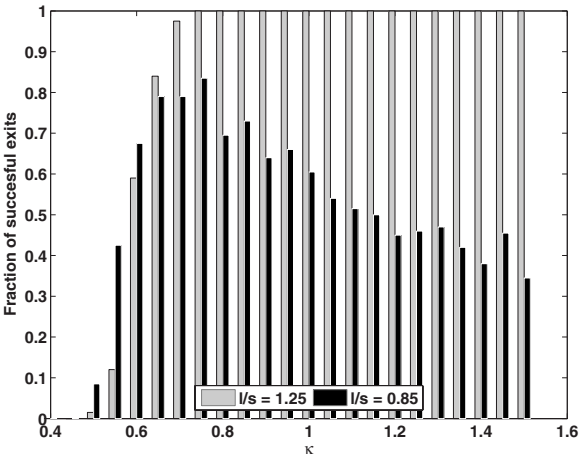

FIG. 8. Fraction of successful exits of the entire chain as a function of the coupling strength κ. The value of the bond length l is given in the legend. The initial conditions are $q_{x0}=-0.05$ and $\Delta q_x=0.001$, yielding $E_0/\Delta E=0.219$. The remaining parameter values are $a=5$ and $N=100$.

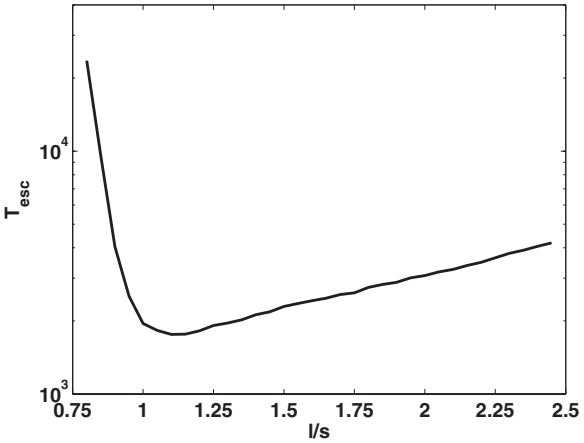

FIG. 9. Mean escape time as a function of the bond length l. The initial conditions are: $q_{x0}=-0.05$ and $\Delta q_x=0.001$, yielding $E_0/\Delta E=0.219$. The remaining parameter values are $a=5$, $\kappa=0.9$, and $N=100$.

reaches there a maximum of 0.835. With further increasing coupling strength the latter curve descends reaching a value of 0.345 at $\kappa=1.5$.

The different shape of the curves can be explained by the dependence of the activation energy on the value of the coupling strength for $l<s$. Here the effective potential barrier that must be overcome during the escape process grows with κ. As a result we observe a drastic reduction of the successful exit events for shorter bond lengths.

B. Dependence of the mean escape time on the bond length

We also study the influence of the bond length on the mean escape time of the oscillator chain. We fix the coupling strength to $\kappa=0.9$, guaranteeing an exit of the entire chain without fragmentation.

The results are shown in Fig. 9. For small bond lengths up to $l/s=1$ the curve drops and at $l/s=1.1$ a minimum is reached. With further increase of the bond length the mean escape time slightly increases.

The rise of the curve for enlarging bond length can be explained with the smaller growth rates of the localized structures created during the process of modulational instability. The effective interaction is weaker. Thus the process of energy localization is slower and thereby all subsequent (exchange) processes induced by the modulational instability are slowed down, too.

VII. DISTRIBUTION OF ESCAPE TIMES

In addition we present the distribution of the escape times for a fixed set of parameter values. Figure 10 shows the distributions obtained from 2×10^4 simulations with different realizations of initial conditions. Interestingly the distribution has periodically recurring peaks. For better illustration an enlargement is presented in the inset of Fig. 10. Let us remind that the chain breathes along its axis with a frequency of $\nu=4.64\times10^{-3}$ for the chosen set of parameter values (cf. Fig. 5), corresponding to a period of about T

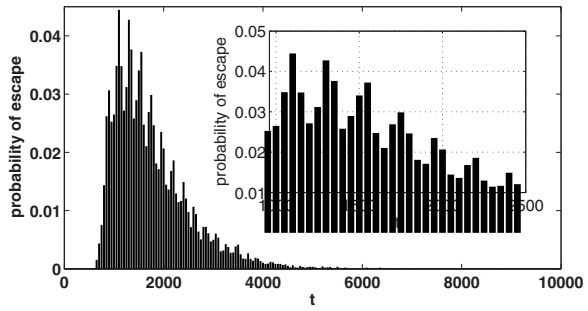

FIG. 10. Distribution of the escape times. The parameter values are $a=5$, $\kappa=0.9$, $l/s=1.25$, and $N=100$. Initial conditions as in Fig. 9. The inset shows a magnification of the histogram for times $1000 \leq t \leq 2500$. The distance between subsequent peaks corresponds to the period of the global oscillations in the y direction.

$=216$. Each time the chain is contracted there are favorable conditions to pass the transition state which for itself involves a narrow configuration in the y direction, cf. Fig. 6. A Fourier analysis of the escape time distribution confirms that the period between two peak appearances, determined as $T=216\pm5$, coincides with the above noted breathing period of the chain $T=216$.

Concerning the dependence of the mean escape time on the average excitation energy, we observe a rather strong decay of T_{esc} with growing ratio $E_0/\Delta E$ in the low-energy region. With further increasing E_0 this decay weakens.

VIII. SUMMARY

In the present work we have considered the conservative and deterministic escape dynamics of a chain of coupled oscillators. Attention has been paid to the barrier crossing of the chain and foregoing processes leading to it when the chain is initially in a flat state near the bottom of a metastable potential.

To be precise, we have considered a two-dimensional spring-mass chain model. Anharmonicity enters our model in a twofold way, first via the expression for the bond length between two adjacent units and second, by the assumption that the oscillators interact via Morse coupling. Each oscillator evolves in a cubic single well potential determining so the transition direction. Initially the energy was homogeneously shared among the units and there was no excitation of the transverse motion.

It has been shown that, starting from this homogeneous lattice state, the system self-promotes an instability of its initial preparation. More precisely, for those lattice states that are modulationally unstable small perturbations grow in the course of time leading to energy localization. In the limiting case of large bond length an analytical estimate for the growth rates of small perturbations of the initial state at an early stage of the dynamics has been presented. The modulational instability of the chain state initiates the appearance of complex lattice dynamics entailing the formation of localized large amplitude breathers in the transition direction on the one hand, and global oscillations in transverse direction on the other hand. Concerning the appearance of large amplitude excitations and the subsequent exit of the chain the critical chain configurations have been presented. We have obtained the surprising result that in the limit of long bonds the activation energy becomes independent of the coupling strength and is equal to the net barrier height.

Furthermore, we pay special interest to the process of energy redistribution due to the excitation of transverse lattice modes. It has turned out that with enhanced interaction strength between the units of the chain the energy flow to the perpendicular motion is accelerated. As a result of these investigations an optimal parameter set offering a fast escape has been derived.

We have presented the distribution of the escape times for a set of parameter values. Recurring peaks of higher probability of escape have been observed. We have linked these peaks to time-periodic structural changes of the chain.

To summarize, even such a complex deterministic system equipped with only a comparatively low amount of energy proved to be able to perform large amplitude excitations with subsequent passing of the transition state. Thus, with respect to the results obtained in [17,18] for the one-dimensional case of harmonically interacting units in the present study we have presented a more elaborate version of the existing concept of deterministic escape processes and thereby offer a wide field of possible applications in physics and biology.

ACKNOWLEDGMENTS

This research has been supported by Contract No. SFB-555 (L.S.-G, S.F.) and by the Volkswagen Foundation Contracts No. I/80424 (P.H.) and No. I/80425 (L.S.-G).

APPENDIX: MODULATIONAL INSTABILITY

For small derivations from the units equilibrium positions the Morse potential can be represented in a harmonic approximation.

According to the initial chain preparation described in Sec. II we look for perturbations of an initially flat mode, i.e., $k_x=0$. We set $q_{yn}(t)=nl$ since we can discard—in a rough approximation—the motion in the y direction for the onset of modulational instability.

Supposing $\Delta q_{xn+1,n}=|q_{xn+1}-q_{xn}| \ll l$—i.e., deviations from the rest positions remain small compared to the equilibrium distance of neighboring units—we expand the square root in (3) as

$$r_{n+1,n} \simeq \sqrt{l^2+\Delta q_{xn+1,n}^2} \simeq l+\frac{\Delta q_{xn+1,n}^2}{2l}. \tag{A1}$$

Eventually we have an equation with a purely nonlinear coupling term,

$$\ddot{q}_{xn}=-q_{xn}+aq_{xn}^2+\frac{\kappa}{2l^2}[(q_{xn+1}-q_{xn})^3-(q_{xn}-q_{xn-1})^3]. \tag{A2}$$

At a very early instant of the dynamics we can consider the small interactions by supposing the following ansatz tak-

ing into account the nonvanishing random perturbations already present in the initial preparation:

$$(q_{xn\pm1}-q_{xn})^3=(q_{xn\pm1}-q_{xn})^2(q_{xn\pm1}-q_{xn}) \lesssim (2\Delta q_x)^2(q_{xn\pm1}-q_{xn}), \tag{A3}$$

with Δq_x as the amplitudes of small random perturbations as introduced in Sec. II. We obtain

$$\ddot{q}_{xn}=-q_{xn}+aq_{xn}^2+\tilde{\kappa}(q_{xn+1}+q_{xn-1}-2q_{xn}). \tag{A4}$$

This equation describes a harmonically coupled chain of oscillators with an effective coupling strength

$$\tilde{\kappa}=2\kappa(\Delta q_x)^2/l^2 \ll \kappa \tag{A5}$$

between adjacent units.

To analyze the nonlinear character of the solutions of Eq. (A4) a nonlinear discrete Schrödinger equation for the slowly varying envelope solution, $Q_n(t)$, has been derived in [27,35],

$$2i\dot{Q}_n+\tilde{\kappa}(Q_{n+1}+Q_{n-1}-2Q_n)+\gamma|Q_n|^2Q_n=0, \tag{A6}$$

with the nonlinearity parameter $\gamma=10a^2/3$. The stability of a plane-wave solution of Eq. (A6) of the form

$$Q_n(t)=Q_0\exp(i\theta_n)+\text{c.c.}, \tag{A7}$$

with $\theta_n=k_xn-\omega t$ (k_x is taken from the first Brillouin zone)—i.e., $k_x\in[-\pi,\pi]$—can be investigated in the weakly nonlinear regime by assuming small perturbations of the amplitude Q_0 and phase θ_n that have the form of sinusoidal modulations with wave number K and frequency Ω. One then finds for the perturbational wave the following dispersion relation [27,35]:

$$[\Omega-\tilde{\kappa}\sin(K)\sin(k_x)]^2=2\tilde{\kappa}\sin^2\left(\frac{K}{2}\right)\cos(k_x) \times\left[2\tilde{\kappa}\sin^2\left(\frac{K}{2}\right)\cos(k_x)-\gamma Q_0^2\right]. \tag{A8}$$

Stability of the perturbations necessitates that Ω is real. Conversely, if the right-hand side of Eq. (A8) is negative the perturbation grows exponentially with a rate

$$\Gamma=\left\{2\tilde{\kappa}\sin^2\left(\frac{K}{2}\right)\cos(k_x)\left[\gamma Q_0^2-2\tilde{\kappa}\sin^2\left(\frac{K}{2}\right)\cos(k_x)\right]\right\}^{1/2}. \tag{A9}$$

Taking into account the weak effective coupling [$\tilde{\kappa}\ll\kappa\sim O(1)$], furthermore setting $k_x=0$, we obtain the following growth rate Γ for perturbations with wave vector Q of the initial flat mode:

$$\Gamma=\sqrt{\tilde{\kappa}\frac{20a^2Q_0^2}{3}\sin^2\left(\frac{K}{2}\right)}+O(\tilde{\kappa}). \tag{A10}$$

Note that the amplitude q_{x0} of the initial state of the system is related to Q_0 via $q_{x0}=2Q_0$.

[1] P. Talkner and P. Hänggi, *New Trends in Kramers' Reaction Rate Theory* (Kluwer Academic, Dordrecht, 1995).
[2] H. Mehrer, *Diffusion in Solids* (Springer-Verlag, New York, 2007).
[3] A. Zettlemoyer, *Nucleation* (Dekker, New York, 1969).
[4] I. Vernik, S. Keil, N. Thyssen, T. Doderer, A. Ustinov, H. Kohlstedt, and R. Huebener, J. Appl. Phys. **81**, 1335 (1997).
[5] H. Kramers, Physica **7**, 284 (1940).
[6] N. van Kampen, *Stochastic Processes in Physics and Chemistry* (Elsevier, Amsterdam, 2004).
[7] P. Hänggi, P. Talkner, and M. Borkovec, Rev. Mod. Phys. **62**, 251 (1990).
[8] V. Mel'nikov, Phys. Rep. **209**, 1 (1991).
[9] J. Langer,Ann. Phys. **54**, 258 (1969).
[10] J. Dunkel, W. Ebeling, L. Schimansky-Geier, and P. Hänggi, Phys. Rev. E **67**, 061118 (2003).
[11] P. J. Park and W. Sung, J. Chem. Phys. **111**, 5259 (1999).
[12] K. L. Sebastian and A. K. R. Paul, Phys. Rev. E **62**, 927 (2000).
[13] K. L. Sebastian, Phys. Rev. E **61**, 3245 (2000).
[14] S. K. Lee and W. Sung, Phys. Rev. E **63**, 021115 (2001).
[15] K. Lee and W. Sung, Phys. Rev. E **64**, 041801 (2001).
[16] P. Kraikivski, R. Lipowsky, and J. Kiefeld, Europhys. Lett. **66**, 763 (2004).
[17] D. Hennig, L. Schimansky-Geier, and P. Hänggi, Europhys. Lett. **78**, 20002 (2007).
[18] D. Hennig, S. Fugmann, L. Schimansky-Geier, and P. Hänggi, Phys. Rev. E **76**, 041110 (2007).
[19] W. Forst, *Theory of Unimolecular Reaction* (Academic, New York, 1971).
[20] S. Flach, Phys. Rev. E **50**, 3134 (1994).
[21] T. Dauxois, M. Peyrard, and C. Willis, Physica D **57**, 267 (1992).
[22] S. Aubry, Physica D **103**, 201 (1997).
[23] S. Flach and C. Willis, Phys. Rep. **295**, 181 (1998).
[24] D. Campbell, S. Flach, and Y. Kivshar, Phys. Today **57**, 43 (2004).
[25] D. Hennig, C. Neißner, M. G. Velarde, and W. Ebeling, Phys. Rev. B **73**, 024306 (2006).
[26] P. Marquié, J. M. Bilbault, and M. Remoissenet, Phys. Rev. E **51**, 6127 (1995).
[27] I. Daumont, T. Dauxois, and M. Peyrard, Nonlinearity **10**, 617 (1997).
[28] T. Dauxois and M. Peyrard, Phys. Rev. Lett. **70**, 3935 (1993).
[29] M. Peyrard, Physica D **119**, 184 (1998).
[30] H. Yoshida, Phys. Lett. A **150**, 262 (1990).
[31] Y. Kivshar and M. Peyrard, Phys. Rev. A **46**, 3198 (1992).
[32] K. W. Sandusky and J. B. Page, Phys. Rev. B **50**, 866 (1994).
[33] M. Toda, *Theory of Nonlinear Lattices* (Springer, Berlin, 1989).
[34] E. Shidlovskaya, L. Schimansky-Geier, and Y. Romanovsky, Z. Phys. Chem. **214**, 65 (2000).
[35] Y. S. Kivshar, Phys. Rev. E **48**, 4132 (1993).